

High-content screening identifies inhibitors of the nuclear translocation of ATF6

CHUN-LEI LIU^{1*}, XIN LI^{1*}, LU GAN^{1*}, YUN-YUN HE¹, LI-LI WANG² and KUN-LUN HE¹

¹Department of Geriatric Cardiology, Chinese PLA General Hospital, Beijing 100853;

²Pharmacy Institute of Military Medical Sciences, Beijing 100850, P.R. China

Received July 16, 2015; Accepted December 11, 2015

DOI: 10.3892/ijmm.2015.2442

Abstract. Activating transcription factor 6 (ATF6) is a transmembrane protein that consists of a cytoplasmic domain and an endoplasmic reticulum (ER) luminal domain. As unfolded protein levels arise in the ER, the ER cytoplasmic domain of ATF6 moves to the nucleus, where it activates the transcription of a range of genes, including those involved in apoptosis. As ATF6 only becomes functional once it has moved to the nucleus, compounds that inhibit its re-localization are of therapeutic interest. The aim of the present study was to rapidly and accurately identify such compounds using a novel image-based, high-content screening (HCS) technique. The results from the HCS analysis were then confirmed by luciferase reporter assays, western blot analysis and the measurement of cell viability. We found that HCS identified compounds which inhibited ATF6 nuclear translocation with high specificity, as confirmed by the luciferase reporter assay and western blot analysis. Moreover, we demonstrated that 3 of the 80 identified compounds impaired ATF6-mediated induced cell death. The data from this study support the theory that HCS is a novel, high throughput method which can be used for accurate and rapid compound screening.

Introduction

Activating transcription factor 6 (ATF6) is an important transcription factor that is involved in the regulation of the endoplasmic reticulum (ER) stress-induced unfolded protein response (UPR) (1,2). When large quantities of unfolded

proteins accumulate in the ER, ATF6 translocates from the ER to the Golgi apparatus, where it is sequentially hydrolyzed by site-1 and -2 proteases (S1P and S2P). Cleaved ATF6 then translocates to the nucleus, where it acts on the ER stress response element (ERSE) to induce the transcription of ER stress-related genes and subsequent ER stress-related cellular responses, including apoptosis (3,4). Previous studies have reported that ER stress and ATF6-activated transcription play a role in the pathogenesis and development of various diseases; these include neurodegeneration, hereditary cerebellar atrophy and ataxia, type 2 diabetes mellitus and diabetic nephropathy, as well as cardiovascular diseases, such as myocardial atrophy, heart failure, ischemic heart disease and atherosclerosis (5-10). Therefore, the inhibition of ATF6-activated transcription may provide a novel therapeutic strategy for the above-mentioned diseases. Indeed, exendin-4 has been shown to attenuate ER stress partly through the inhibition of ATF6-mediated transcription (11). Nucleobindin-1 was also found to control the UPR by inhibiting ATF6 activation (12). Citron *et al* reported that the inhibitor of ATF6, 4-(2-aminoethyl)-benzenesulfonyl fluoride (AEBSF), inhibited the production of amyloid β -protein, which is an early and critical characteristic of Alzheimer's disease (13).

One method for screening inhibitors of ATF6 nuclear translocation/activation involves the ATF6-activated expression of the luciferase reporter gene; this requires the use of ERSE-containing promoters fused with the luciferase reporter gene (14). The activity of ATF6 can then be deduced from the light intensity of luciferase. An alternative indirect method involves the quantification of the cellular levels of ATF6 and related proteins by western blot analysis (15). Recently, high-content screening (HCS) has emerged as a novel technology for the high throughput screening of drugs. It allows for the quantitative and multi-parametric analysis of living cells in a single experiment (16). Specifically, the biological activities and cytotoxicity of tested compounds can be monitored simultaneously. Thus, HCS has remarkable advantages over other drug-screening techniques. Using HCS analytical techniques, the effect of various pharmacological treatments on the nuclear-cytoplasm distribution of ATF6 may be quantified. Hence, the information concerning ATF6 activation and activities of the pharmacological agents can be obtained. Furthermore, the selectivity of the tested compounds on ATF6 activation may be verified using information, such as cellular and nuclear morphologies.

Correspondence to: Dr Kun-Lun He, Department of Geriatric Cardiology, Chinese PLA General Hospital, 28 Fuxing Road, Beijing 100853, P.R. China

E-mail: hekl301@aliyun.com

Dr Li-Li Wang, Pharmacy Institute of Military Medical Science, 27 Taiping Road, Beijing 100850, P.R. China

E-mail: wangll63@126.com

*Contributed equally

Key words: high-content screening, nuclear translocation assay, activating transcription factor 6, endoplasmic reticulum stress

In this study, we employed the HCS technique to screen for inhibitors of ATF6 activation. The reliability of HCS was also validated by luciferase reporter assay and western blot analysis. Finally, the effectiveness of the screened compounds was tested by cellular viability assays.

Materials and methods

Compounds and cell lines. PP1-01 to PP1-80 were synthesized (Fig. 1) at the Beijing Institute of Pharmacology and Toxicology based on salubrinal (Beijing, China). U2OS osteosarcoma cells stably expressing ATF6-enhanced green fluorescent protein (ATF6-EGFP) were obtained from Thermo Scientific (Lafayette, CO, USA). The cells were grown in Dulbecco's modified Eagle's medium (DMEM; Gibco-Life Technologies, Carlsbad, CA, USA) containing 10% fetal bovine serum (FBS; Thermo Scientific HyClone, Waltham, MA, USA), 2 mM L-glutamine (Sigma, St. Louis, MO, USA) and 0.5 mg/ml G418 (Merck, Darmstadt, Germany). H9C2 myocardial cells were purchased from the cell bank of Peking Union Medical College Hospital (Beijing, China). The cells were grown in DMEM containing 10% FBS. All cells were incubated at 37°C in 5% CO₂ incubator.

HCS detection of nuclear translocation. The cells were seeded in black, clear-bottomed, cell culture-treated 96-well plates (Corning Inc., Corning, NY, USA) at a density of 10⁴ cells/well in 100 µl growth medium. The plates were then briefly vortexed and centrifuged to aid the release of trapped air bubbles and to facilitate the even dispersal of cells within each well. The cells were then allowed to attach and grow for 24 h in DMEM containing 10% FBS, 2 mM L-glutamine and 0.5 mg/ml G418. The following day, the culture medium was replaced with species medium. The species medium contained DMEM (high glucose) with 1% FBS, 2 mM L-glutamine, and 0.5 mg/ml G418. The plates were then incubated for 5 h prior to the addition of 50 µl/well of the 4X concentrated test compound and 10 µl/well of 4X tunicamycin (TM; final concentration 1 µM; Merck) for 5 h. Subsequently, 100 µl 3X fixation solution, which contained 11.1% formaldehyde and 1 µM Hoechst 33342 (Sigma) diluted in PBS, was added to each well and the plates were incubated at room temperature for 20 min. The final concentrations of the fixing and staining agents in the assay plate wells were 3.7% formaldehyde and 1 µg/ml Hoechst 33342 dye. The plates were then washed 3 times with PBS and sealed with easy-peel foil using a plate sealer. In the primary screening, only 2 concentrations of the compounds were tested: 3 and 30 µM. In the dose-related screening, the compounds were assayed at 5 concentrations: 0.3, 1, 3, 10 and 30 µM. All compounds were tested in triplicate.

Fluorescent images were acquired using an IN Cell Analyzer 1000 platform (GE Healthcare, Cleveland, OH, USA). Specifically, 5 fields in the center of each well were selected and imaged through both blue and green channels. The blue channel images were acquired using 360/40-nm excitation and 460/40-nm emission filters with a 300-msec exposure time. The green channel images were acquired using 475/20-nm excitation and 535/50-nm emission filters with an 800-msec exposure time. The IN Cell Analyzer 1000 was set up to acquire 5 fields-of-view. Image analysis was performed using the cell analysis software of the IN Cell Analyzer 1000 Workstation 3.5. For each

cell, the GFP fluorescence intensity in the nuclear circle and cytoplasmic ring was measured and divided by the respective area of the cell, to yield the average fluorescence intensity for each region. We evaluated the ratio of nuclear-to-cytoplasmic GFP fluorescence intensity to quantify nuclear localization (N/C). The inhibitory ratio (activity) was calculated relative to the controls (untreated cells) using the following formula: activity (%) = [TM signal (N/C) - compound signal (N/C)]/[TM signal (N/C) - control (N/C)] x100. Based on the dose-response curve, the R² and IC₅₀ values were calculated.

Luciferase reporter assay. The reporter vectors, pGL4.39 (luc2P/ATF6-RE/Hygro) and pGL4.75 (hRluc/CMV), and the Dual-Glo[®] Luciferase assay system were obtained from Promega (Madison, WI, USA). We used X-tremeGENE HP to transfect the U2OS cells with the reporter plasmid (6 µg) pGL4.39 (luc2P/ATF6-RE/Hygro) and the control pGL4.75 (hRluc/CMV) vector according to the manufacturer's instructions. Subsequently, the cells were seeded into black, clear-bottomed, cell-culture treated 96-well plates (Corning, Inc.) at a density of 10⁴ cells/well in 100 µl growth medium. Following overnight incubation, the medium was changed to species medium containing DMEM (high glucose) with 0.5% charcoal-stripped FBS and 2 mM L-glutamine, and the cells were incubated for 24 h. Following incubation, the plates were allowed to cool to room temperature for 10 min prior to the addition of 100 µl Dual-Glo[®] luciferase reagent to each well. Luminescence was then measured using a Fluorescence plate reader (BioTek Instruments, Winooski, VT, USA) and data were normalized to in-plate controls. After at least a 10-min wait, 100 µl Dual-Glo[®] Stop and Glo[®] reagent was added to each well to measure *Renilla* luminescence. We evaluated the firefly and *Renilla* fluorescence intensity for each well in order to measure promoter activity and cytotoxicity, respectively, and used firefly/*Renilla* to yield results.

The inhibitory ratio (activity) was calculated relative to the controls (untreated cells) using the following formula: activity (%) = [TM signal (firefly/*Renilla*) - compound signal (firefly/*Renilla*)]/[TM signal (firefly/*Renilla*) - control (firefly/*Renilla*)] x100. Based on the dose-response curve, the R² and IC₅₀ values were calculated.

Western blot analysis. The H9C2 cells were inoculated in 6-well plates at 10⁶ cells/well, and exposed to the different compounds for 30 min prior to treatment with TM for 24 h. The cells were then lysed in whole cell lysis buffer [62.5 mM Tris-HCl (pH 6.8 at 25°C) and 2% w/v sodium dodecyl sulfate (SDS), 10% glycerol and 50 mM DTT]. The homogenates were heated in a 100°C water bath for 10 min and then centrifuged at 12,000 x g for 10 min at 4°C. We then used the BCA method to determine the protein concentration of each sample. Equal amounts of cellular proteins were subsequently separated by electrophoresis on 10% SDS-polyacrylamide gels and transferred onto PVDF membranes. After blocking (1X TBS, 0.1% Tween-20 and 5% w/v non-fat dried milk), the membranes were incubated with antibodies to ATF6 (1:1,000; ab11909), GRP78 (1:100; ab21685) (all from Abcam, Cambridge, UK) and GAPDH (1:1,000; TA-08; Zhongshan Golden Bridge Biotechnology, Beijing, China) with gentle agitation overnight at 4°C. Subsequently, the membranes were incubated with the

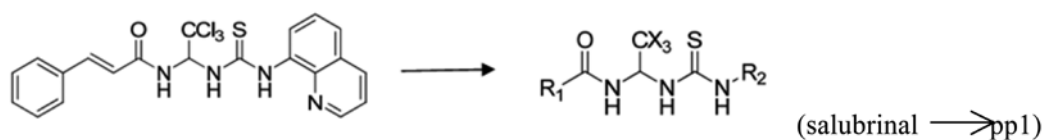


Figure 1. Chemical structure and synthesis of the compounds PPI-01 to PPI-80.

appropriate horseradish peroxidase-conjugated secondary antibodies [anti-mouse (ZDR-5117), anti-rabbit (ZDR-5118); Zhongshan Golden Bridge Biotechnology] at a 1:5,000 dilution for 1 h at room temperature. The membranes were then incubated with enhanced chemiluminescence (ECL) reagents, exposed to film and developed. Finally, the film was scanned with an imaging densitometer (AlphaImager 5500; Alpha Innotech, San Leandro, CA, USA), and the optical density was quantified using Multi-Analyst software.

Methylthiazol tetrazolium (MTT) assay. The H9C2 cells were seeded in a 96-well plate at 10^4 cells/well and treated with various concentrations (0.3, 1, 3, 10 and 30 μ M) of the test compounds (PPI-13, PPI-14 and PPI-19) 30 min prior to treatment with TM (1 μ M). The compounds were dissolved in dimethyl sulfoxide (DMSO; Amresco, Solon, OH, USA). Forty-eight hours later, 10 μ l of 5 mg/ml MTT were added to each well for 4 h; the supernatants were then removed and replaced with 100 μ l DMSO. Following gentle agitation for 10 min, the absorbance value of each well was measured at 550 nm using a universal microplate reader (BioTek Instruments). The relative number of viable cells was determined by comparison with untreated cells, in which viability was assumed to be 100%.

Ultrastructure analysis. The H9C2 cells were fixed in cold 2,5-glutaraldehyde in 0.1 mol/l cacodylate buffer (pH 7.3), post-fixed in 1% OsO_4 , dehydrated and embedded in Epon. Ultrathin sections were mounted on copper grids, stained with uranyl acetate and lead citrate, and examined under a Jem-100C (Jeol, Tokyo, Japan) electron microscope. Electron micrographs were taken systematically at $\times 1,000$ magnification.

Statistical analysis. Each experiment was repeated at least 3 times, and values are presented as the means \pm SD. Statistical analyses were performed by a one-way analysis of variance (ANOVA). A P-value <0.05 was considered to indicate a statistically significant difference.

Results

Detection of inhibitors of ATF6 nuclear translocation by HCS. Under normal conditions, ATF6 is primarily located in the cytoplasm. TM can activate ATF6, which results in its accumulation in the nucleus (3). In this study, we examined the effects of various compounds on the TM-induced ATF6 cytoplasmic-nuclear translocation. Fig. 2 shows representative images of cytoplasmic and nuclear and cytoplasmic fluorescence signals recorded in the U2OS cells expressing ATF6-EGFP under control (DMSO) or TM-treated conditions and in the presence of the test compounds. Upon manual inspection, 15 compounds (PPI-10, 11, 12, 18, 22, 32, 37, 58, 62,

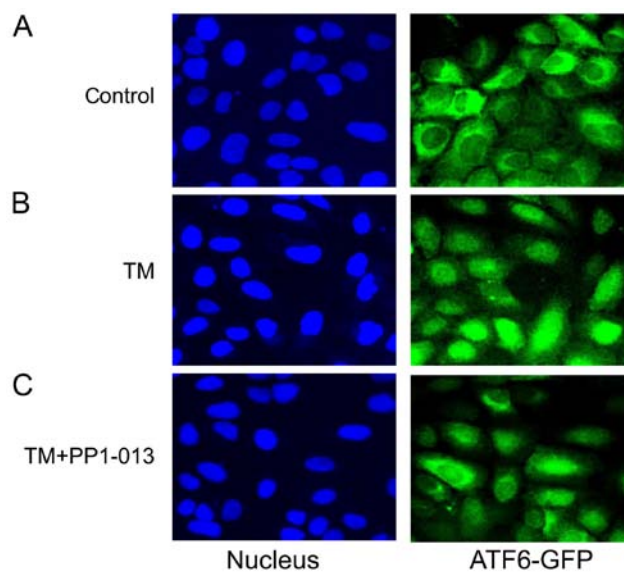


Figure 2. Representative images of U2OS cells expressing active transcription factor 6 (ATF6)-green fluorescent protein (GFP) in the different groups. (A) In the control group, ATF6 was primarily located in the cytoplasm. (B) In the group treated with tunicamycin (TM) (1 μ M) only, ATF6 translocated to the nucleus. (C) In the presence of the compounds (30 μ M PPI-013) and TM (1 μ M), ATF6 translocation to the nucleus was partly inhibited.

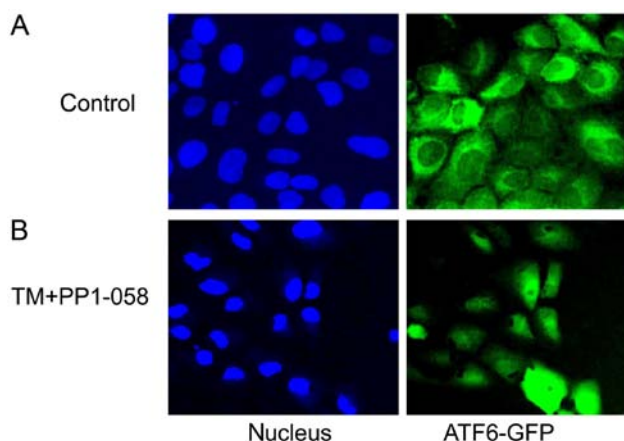


Figure 3. Representative images of U2OS cells expressing normal and abnormal active transcription factor 6 (ATF6)-green fluorescent protein (GFP). (A) The flat shape of ATF6-GFP-U2OS cells in the control group can be noted. (B) The cells were rounded phenotypes in compounds (30 μ M PPI-058) with toxicity.

65, 69, 70, 74, 75, 76) were initially excluded from the analysis, as it was determined that false-positive results were reported. Indeed, by contrast to the normally very flat U2OS cell shape, the cells exposed to these compounds exhibited a rounded phenotype and caused false-positives, as the cytoplasm and nucleus were not as spatially distinct (Fig. 3).

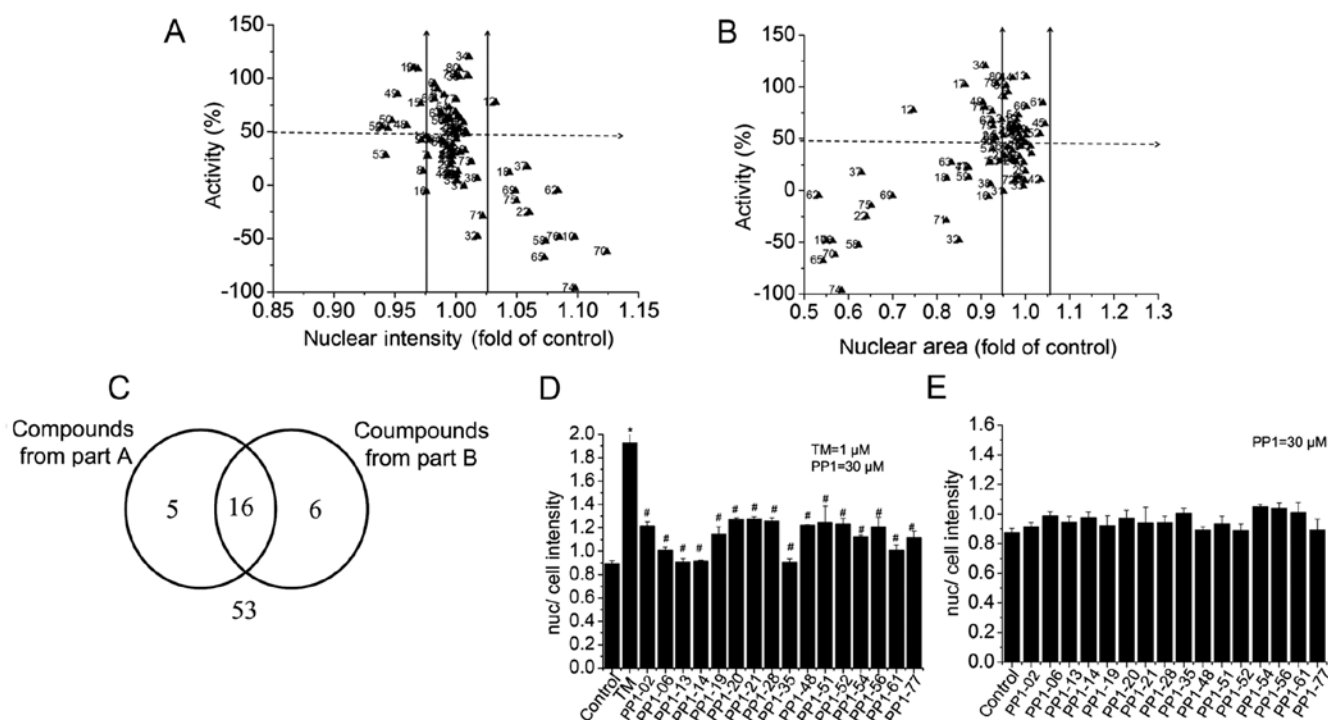


Figure 4. Effective compounds were identified by primary screening. Cells were treated with the different compounds for 30 min prior to exposure to tunicamycin (TM) for 24 h. Nuclear intensity and area were normalized to the control. 'Activity' denotes the active transcription factor 6 (ATF6)-green fluorescent protein (GFP) nucleus (Nuc)-cytoplasm (Cyto) difference normalized to positive and negative controls. The compounds with activity >50% with a nuclear intensity between 0.975 (1.025 and nuclear area between 0.95) and 1.05 were identified as effective for further examination. (A) The distribution of nuclear intensity and activity of the 80 compounds. (B) The distribution of nuclear area and activity of 80 compounds. (C) Venn diagram of compounds identified shown in (A) and (B). For a list of effective compounds identified [shown in (A) and (B)], refer to Table I. (D) Compounds attenuated the increased Nuc/Cell intensity induced by TM. * $P < 0.05$ vs. control; # $P < 0.05$ vs. TM-treated cells. (E) Compounds themselves exert no significant effect on Nuc/Cell intensity. $P > 0.05$ for the comparison between compounds only groups and control.

For the primary screening, each compound was tested at 2 concentrations, 0.3 and 3 μM . During the test, Z' based was 0.603, which was consistently >0.3 and thus suitable for screening. 'Activity' is the ATF6-GFP nucleus (Nuc)-cytoplasm (Cyto) difference normalized to the positive [TM signal (N/C)] and negative [control (N/C)] controls. The compounds with activity <50% had no effect. Compared with the control, nuclear intensity increased and nuclear area decreased eliminates cytotoxic. Of the 80 compounds tested, 16 compounds decreased the nuclear fluorescence of ATF6 by >50% activity with a nuclear intensity ranging from 0.975 to 1.025-fold less than that of the TM-only control. Moreover, 21 compounds decreased nuclear fluorescence >50% activity, with a nuclear area ranging from 0.95 to 1.05-fold less than that of the TM-only control. Determination of the compounds which overlapped for both reduced intensity and area resulted in 16 candidate compounds with >50% activity that were used for further examination (Fig. 4 and Table I).

Dose-response analysis of candidate compounds by HCS.

In order to evaluate the dose response of the 16 candidate compounds that inhibited ATF6 nuclear translocation, the nuclear and cytoplasmic fluorescence profiles were recorded after applying the different concentrations of the compounds by HCS. We found that 3 of the 16 candidate compounds inhibited the TM-induced ATF6 localization to the nucleus in a dose-dependent manner. PP1-13, PP1-14 and PP1-19 showed 50% inhibitory concentrations (IC_{50}) of 5.04, 2.89

and 16 $\mu\text{mol/l}$, respectively, and R^2 values of 0.91, 0.94 and 0.92, respectively. The inhibition of ATF6 localization to the nucleus was only 2.48% with PP1-13 at a concentration of 0.3 μM ; however, this effect increased up to 90.38% at 30 μM (Fig. 5 and Table II).

Dose-response analysis of candidate compounds by luciferase assay. To validate the compounds identified by HCS, a luciferase assay was performed. Compared with the control, TM increased ATF6-driven activation of luciferase activity. By contrast, the candidate compounds impaired this effect in a dose-dependent manner. The IC_{50} values of PP1-13, PP1-14 and PP1-19 were 4.17, 2.54 and 16.59 $\mu\text{mol/l}$, respectively; the R^2 values were 0.94, 0.86 and 0.60, respectively. PP1-13, for example, exhibited a mean inhibitory activity of 43.59%; however, the compound attained up to 99.95% inhibition of TM-induced ATF6-driven luciferase activity at a concentration of 30 μM , when compared with the effects of TM alone (Fig. 5).

Effect of the candidate compounds on the protein expression levels of cleaved (cle) ATF6, GRP78 and p-eIF2 α in H9C2 cells. To further confirm the results obtained by HCS and luciferase assay, western blot analysis was performed to detect the expression of cleaved-ATF6 protein and that of its downstream target, GRP78, in H9C2 cells. Compared with the untreated controls, the cleaved ATF6 and GRP78 expression levels were significantly increased in the cells treated

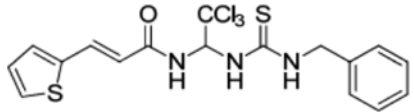
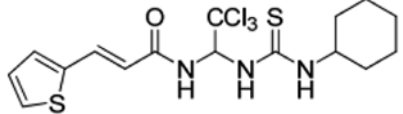
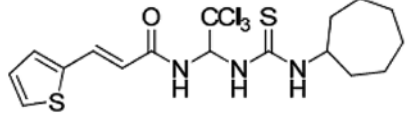
Table I. Compounds identified by primary screening.

Compound	Concentration (μM)	Activity (%)
PP1-02	3	38.44
	30	62.87
PP1-06	3	82.87
	30	95.17
PP1-13	3	27.45
	30	110.05
PP1-14	3	104.89
	30	109.04
PP1-19	3	58.61
	30	68.54
PP1-20	3	10.07
	30	53.14
PP1-21	3	21.79
	30	52.46
PP1-28	3	20.21
	30	54.93
PP1-35	3	26.76
	30	101.49
PP1-48	3	3.74
	30	56.15
PP1-51	3	16.50
	30	53.15
PP1-52	3	11.12
	30	54.59
PP1-54	3	46.87
	30	72.84
PP1-56	3	72.81
	30	60.10
PP1-61	3	19.87
	30	84.80
PP1-77	3	64.67
	30	80.25

with TM. By contrast, exposure to the different candidate compounds impaired the effects of TM and instead returned the expression levels of ATF6 and GRP78 to close to the basal levels (Fig. 6A and B). To evaluate the possible mechanisms through which the screened compounds inhibited ATF6 activation, the phosphorylation of eIF2 α was detected. Compared with the untreated controls, p-eIF2 α expression was increased in the cells treated with TM. Compared with the cells treated with TM, exposure to the different candidate compounds further increased the phosphorylation levels of eIF2 α (Fig. 6C).

Effects of the candidate compounds on the viability of H9C2 cells. To further examine the effects of the candidate

Table II. Structure of the effective compounds detected using the HCS technique.

Compounds	Structure
PP1-13	
PP1-14	
PP1-19	

HCS, high-content screening.

compounds, their effects on cell viability were measured by MTT assay using the H9C2 cells. Compared with the untreated controls (100%), viability was only 46.63% in the cells treated with TM. However, co-treatment with TM and the different candidate compounds significantly increased cell viability. For example, in the H9C2 cells exposed to 10 and 30 μM PP1-13, the viability increased up to 76.772 and 80.93%, respectively (Fig. 7A). Cell viability assay demonstrated no significant differences between the cells treated with the compounds only and the controls (Fig. 7B).

Effects of the candidate compounds on the ultrastructure of H9C2 cells. The microstructure of the nucleus was examined by electron microscopy. Treatment with TM resulted in very convoluted nuclei with chromatin margination. Following exposure to PP1-13, PP1-14 and PP1-19, margination aggregation disappeared (Fig. 8)

Discussion

Considering the role of ATF6-associated pathways in the development of numerous diseases, ATF6 is an attractive candidate drug target (18,19). Thus, in this study, to identify compounds that inhibit ATF6 translocation, we used HCS. We used the U2OS cell line, stably expressing ATF6-EGFP, as our model for HCS, whereas TM was used to activate its nuclear translocation. We then screened 80 novel compounds, developed from a target-based drug design, and found that 3 of these small molecules inhibited the TM-induced nuclear translocation of ATF6. The reliability of the HCS approach was further corroborated by conventional methods, including luciferase reporter gene assay, western blot analysis and finally the measurement of cell viability.

Using HCS, we concluded that 3 compounds inhibited the nuclear translocation of ATF6 in a dose-dependent manner. The R^2 values of the 3 compounds were all >0.9 , while the IC_{50} values ranged from 2.89-16 $\mu\text{mol/l}$, which are relatively

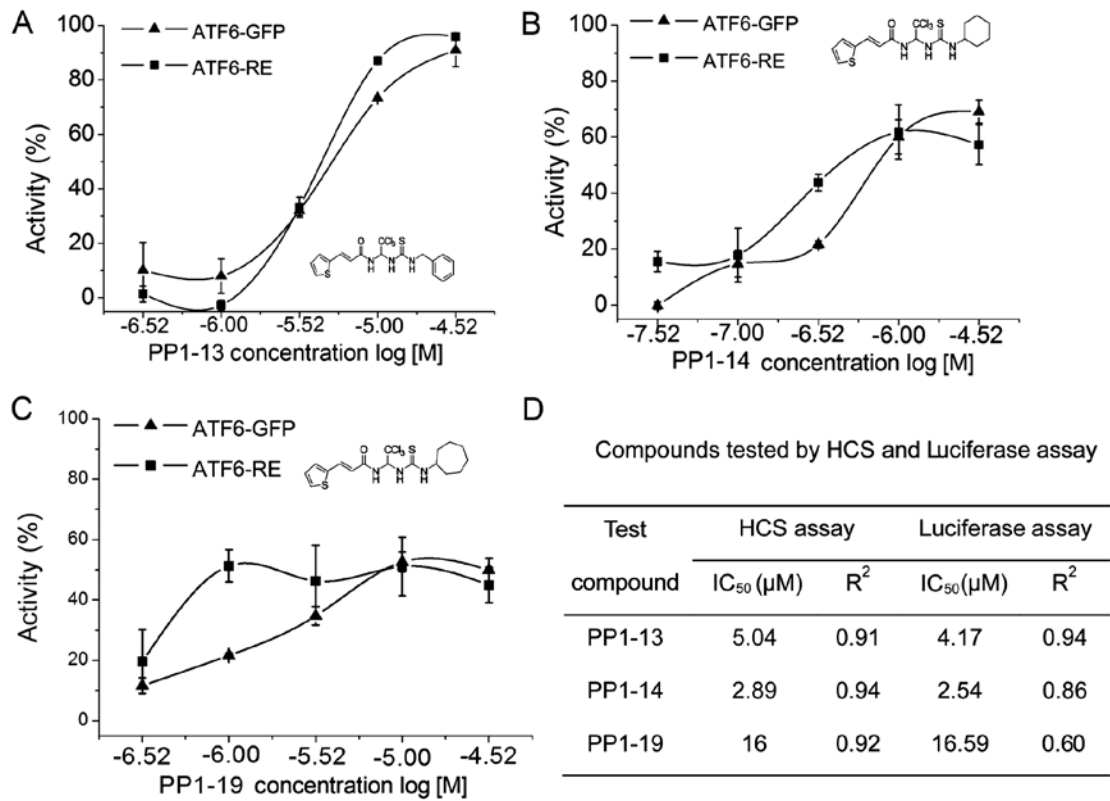


Figure 5. Comparison of active transcription factor 6 (ATF6)-green fluorescent protein (GFP), high-content screening (HCS) and ATF6-RE luciferase reporter assay by concentration response effects of preferred compounds. Cells were treated with DMSO, tunicamycin (TM) (1 μM) or the different compounds at various concentrations (0.3, 1, 3, 10 and 30 μM). Nuclear translocation was detected by HCS and ATF6-RE luciferase reporter assay, respectively. ‘Activity’ is the ATF6-GFP nucleus (Nuc)-cytoplasm (Cyto) difference normalized to positive and negative controls in the HCS assay. ‘Activity’ is the ATF6-RE firefly-*Renilla* difference normalized to positive and negative controls in the ATF6-RE luciferase reporter assay. The values represent the average of 3 wells; error bars denote the standard deviation. (A) PP1-13; (B) PP1-14; (C) PP1-19; (D) table of IC₅₀ values and R² tested by HCS and ATF6-RE luciferase reporter assay.

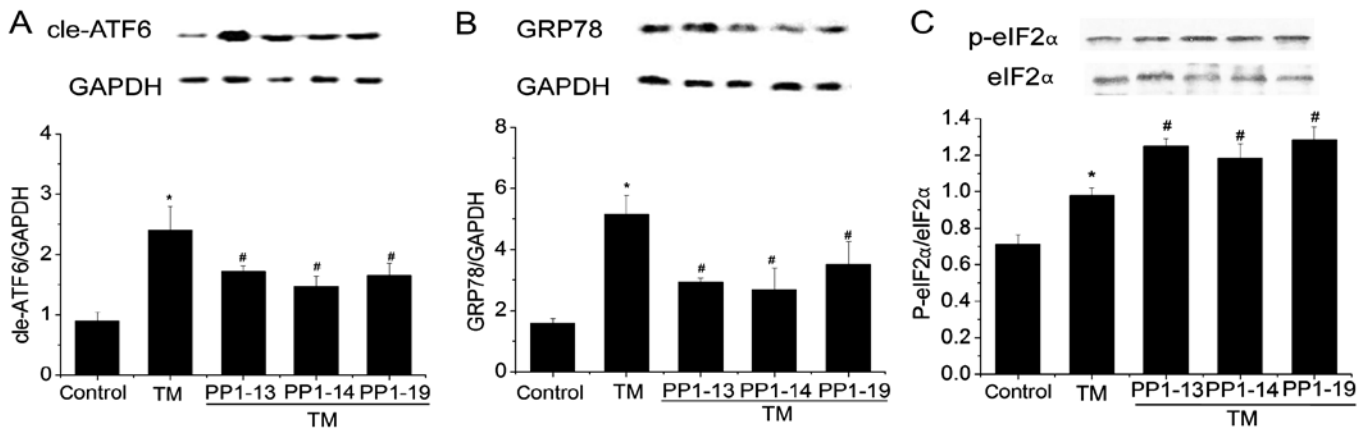


Figure 6. Expression of active transcription factor 6 (ATF6) and GRP78 in H9C2 cells. H9C2 cells were inoculated with the different compounds (PP1-13, PP1-14 and PP1-19) 30 μM for 30 min prior to treatment with tunicamycin (TM) (1 μM) for 24 h. (A) cleaved (cle) ATF6/GAPDH. (B) GRP78 expression. (C) p-eIF2α/eIF2α expression in H9C2 cells. The lower panels depict the mean data, and results are shown as the means ± SEM. *P<0.05 vs. control; #P<0.05 vs. TM.

low, suggesting that these compounds are therapeutically applicable. To confirm the results from HCS, we used the luciferase reporter gene assay to determine whether the 3 identified compounds impaired ATF6-dependent luciferase gene transcription. The results were consistent with those of HCS. Although both methods were able to select compounds which effectively impaired the TM-induced ATF6 translocation/activation, the R² values obtained by the HCS method

were generally higher than those obtained from the luciferase reporter assays, thus demonstrating its greater sensitivity. As the above two approaches used ATF6-overexpressing U2OS cells, we further examined the inhibitory effects of the active compounds on endogenous ATF6 in the myocardial cell line, H9C2. The results revealed that the 3 identified compounds inhibited both TM-induced ATF6 protein expression and that of its downstream target. This further corroborates

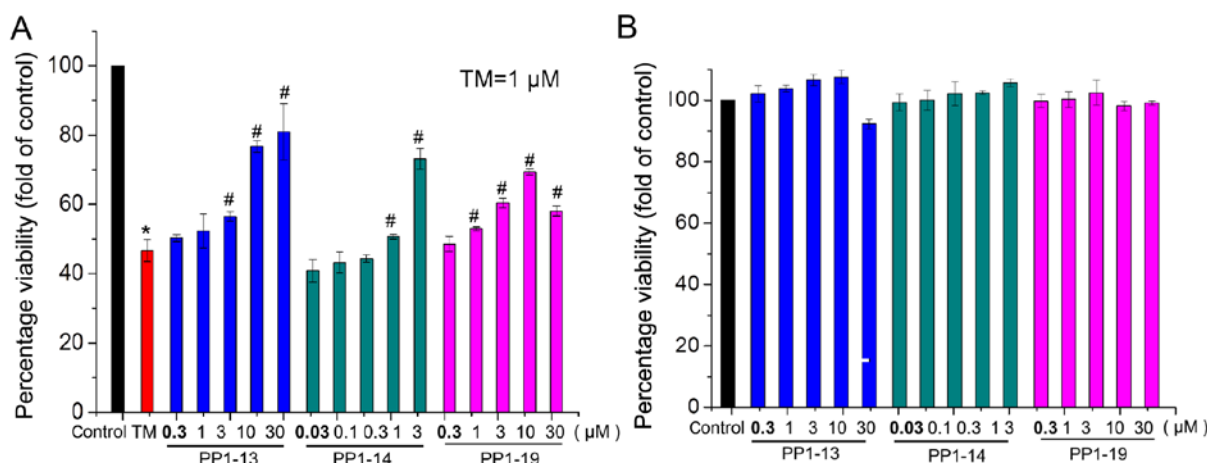


Figure 7. Preferred compounds protect cardiomyocytes against cytotoxicity induced by tunicamycin (TM). Cultured neonatal rat cardiomyocytes were exposed to the different compounds (PP1-13, PP1-14 and PP1-19) for 30 min prior to exposure to TM (1 μ M) for 48 h. Cell viability was then measured as described in the Materials and methods by MTT assay. (A) Viability of cells treated with TM and the different compounds. (B) Viability of cells treated with compounds only. 'Viability' is normalized to controls. *P<0.05 vs. control; #P<0.05 vs. TM.

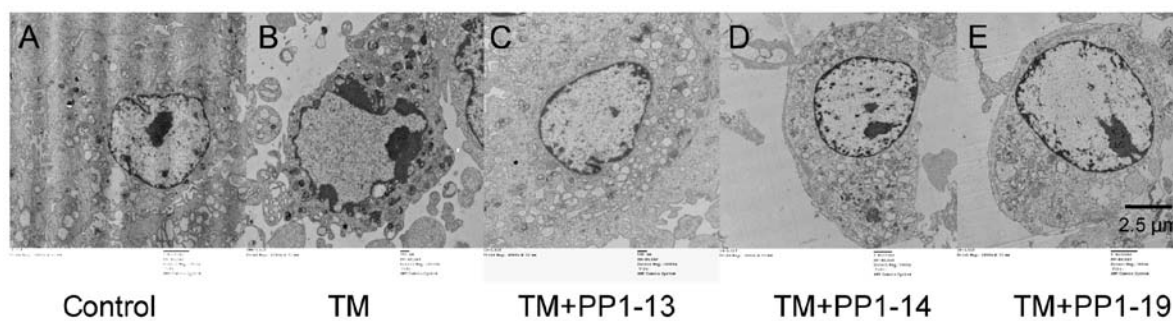


Figure 8. Ultrastructure of cardiomyocytes treated with or without screened compounds. (A) Ultrastructure of normal cardiomyocytes nuclear in the control group. Ultrastructure of cardiomyocyte nuclei in the group treated with tunicamycin (TM) (1 μ M). Convoluted nuclei with chromatin margination are visible. (B) Normal types of ER disappeared, instead of accumulation of lysosomal. Ultrastructure of cardiomyocyte nuclei in 30 μ M PP1-013, 3 μ M PP1-014 and 30 μ M PP1-019-treated groups. Marginal aggregation caused by TM disappeared in these groups. (C-E) Normal types of ER reappeared and accumulation of lysosomal disappeared.

the theory that active compounds identified by HCS are inhibitors of ATF6. As salubrinal was first shown to protect PC-12 cells from ER stress through the selective inhibition of eIF2 α dephosphorylation (20), we detected whether these screened compounds exerted the same protective effects. The results demonstrated that the screened compounds further increased eIF2 α phosphorylation. These results suggest that these screened compounds enhanced eIF2 α phosphorylation, which attenuated translation initiation and reduced protein synthesis to allow cells to clear unfolded proteins and inhibit ATF6 activation. Finally, we examined the cytoprotective effects of the active compounds on H9C2 cells. The results revealed that the HCS-identified compounds exerted significant protective effects against ATF6-induced cell death in the H9C2 cells treated with TM. Moreover, the screen-identified compounds attenuated the margination aggregation induced by TM. These results also validated our theory that HCS is a reliable method for the selection of effective ATF6 inhibitors.

From a technical perspective, western blot analysis is widely used to quantify protein expression. Nevertheless, western blot analysis can be a tedious and time-consuming method. Moreover, western blot analysis only provides output concerning total cell responses, and cannot indicate the subcel-

lular origins of the responses (21). The transcription factor activated luciferase reporter gene assay is a method for quantifying target specific transcriptional activation by transcription factors. However, one shortcoming is that it is necessary to lyse cells to extract luciferase, in order to acquire information (22). Thus, they are not suitable for *in vivo* cellular analysis. Moreover, the two methods offer only limited data; specifically, they cannot reveal the complete picture of the biological activities of screened molecules. HCS is a novel technique in high throughput drug screening which allows for direct observation of the effects of tested compounds on morphology, structure and toxicity in living cells (23). Through the use of an automated graphical analysis system in HCS, multiple parameters, including cellular morphology and fluorescent label distribution and intensity can be more objectively and quantitatively monitored. Indeed, both biological activities and toxicities of tested agents can be monitored at the same time, and thus HCS provides more reliable data than those obtained via other methods (24,25). Moreover, the quantities of cells used are small and the steps are largely automated (26). In short, compared with the reporter gene assay or western blot analysis, the HCS protocol reported in the current study is simpler and more efficient.

The HCS and luciferase assay both identified compounds which impaired ATF6 nuclear translocation at a concentration of approximately 10 μ mol/l. These data are consistent with those of another study that tested these types of compounds (27). As the compounds were synthesized on the basis of salubrinal, these results indicated the consistent efficiency of these screened compounds compared with salubrinal. Of note, the active compounds identified by HCS were observed to share a similar structure, which is consistent with our previous study (17). Notably, there are some disadvantages in our current study. First, we selected U2OS cells, a cell model engineered to highly express exogenous ATF6-EGFP for image capturing. In future studies, cells with endogenous expression of ATF6 should be used for HCS analysis. Second, the association between compound structures and how they contribute to the impairment of ATF6 nuclear translocation remains unknown. Thus, other structure-based assays are warranted to elucidate the exact functions of these compounds and their mechanisms of action.

In conclusion, the HCS protocol used in the current study efficiently detected compounds that inhibited ATF6 activation. The reliability of the protocol was corroborated by luciferase reporter gene assay and western blot analysis. We identified 3 compounds which inhibited ATF6 nuclear translocation and impaired ATF6-mediated induced cell death. Thus, HCS may be valuable in future applications concerning ATF6 activation and activities of the related pharmacological agents.

Acknowledgements

This study was funded by the Ministry Science Foundation of the Chinese People's Liberation Army during the 12th Five-Year Plan Period (no. BWS12J048) and the Major International Science and Technology Cooperation Projects (no. 2013DFA31170).

References

- Wiseman RL and Balch WE: A new pharmacology - drugging stressed folding pathways. *Trends Mol Med* 11: 347-350, 2005.
- Wiseman RL, Haynes CM and Ron D: SnapShot: the unfolded protein response. *Cell* 140: 590-590.e2, 2010.
- Hong M, Luo S, Baumeister P, Huang JM, Gogia RK, Li M and Lee AS: Underglycosylation of ATF6 as a novel sensing mechanism for activation of the unfolded protein response. *J Biol Chem* 279: 11354-11363, 2004.
- Zhao L and Ackerman SL: Endoplasmic reticulum stress in health and disease. *Curr Opin Cell Biol* 18: 444-452, 2006.
- Boot-Handford RP and Briggs MD: The unfolded protein response and its relevance to connective tissue diseases. *Cell Tissue Res* 339: 197-211, 2010.
- Northington FJ, Chavez-Valdez R and Martin LJ: Neuronal cell death in neonatal hypoxia-ischemia. *Ann Neurol* 69: 743-758, 2011.
- Mei J and Niu C: Alterations of Hrd1 expression in various encephalic regional neurons in 6-OHDA model of Parkinson's disease. *Neurosci Lett* 474: 63-68, 2010.
- Chu WS, Das SK, Wang H, Chan JC, Deloukas P, Froguel P, Baier LJ, Jia W, McCarthy MI, Ng MC, *et al*: Activating transcription factor 6 (ATF6) sequence polymorphisms in type 2 diabetes and pre-diabetic traits. *Diabetes* 56: 856-862, 2007.
- Vekich JA, Belmont PJ, Thuerlauf DJ and Glembofski CC: Protein disulfide isomerase-associated 6 is an ATF6-inducible ER stress response protein that protects cardiac myocytes from ischemia/reperfusion-mediated cell death. *J Mol Cell Cardiol* 53: 259-267, 2012.
- Hotamisligil GS: Endoplasmic reticulum stress and the inflammatory basis of metabolic disease. *Cell* 140: 900-917, 2010.
- Lee J, Hong SW, Park SE, Rhee EJ, Park CY, Oh KW, Park SW and Lee WY: Exendin-4 attenuates endoplasmic reticulum stress through a SIRT1-dependent mechanism. *Cell Stress Chaperones* 19: 649-656, 2014.
- Tsukumo Y, Tomida A, Kitahara O, Nakamura Y, Asada S, Mori K and Tsuruo T: Nucleobindin 1 controls the unfolded protein response by inhibiting ATF6 activation. *J Biol Chem* 282: 29264-29272, 2007.
- Citron M, Diehl TS, Capell A, Haass C, Teplow DB and Selkoe DJ: Inhibition of amyloid beta-protein production in neural cells by the serine protease inhibitor AEBSF. *Neuron* 17: 171-179, 1996.
- Damiano F, Tocci R, Gnoni GV and Siculella L: Expression of citrate carrier gene is activated by ER stress effectors XBP1 and ATF6 α , binding to an UPRE in its promoter. *Biochim Biophys Acta* 1849: 23-31, 2015.
- Cox DJ, Strudwick N, Ali AA, Paton AW, Paton JC and Schröder M: Measuring signaling by the unfolded protein response. *Methods Enzymol* 491: 261-292, 2011.
- Bouck DC, Shu P, Cui J, Shelat A and Chen T: A high-content screen identifies inhibitors of nuclear export of forkhead transcription factors. *J Biomol Screen* 16: 394-404, 2011.
- Liu J, He KL, Li X, Li RJ, Liu CL, Zhong W and Li S: SAR, cardiac myocytes protection activity and 3D-QSAR studies of salubrinal and its potent derivatives. *Curr Med Chem* 19: 6072-6079, 2012.
- Toko H, Takahashi H, Kayama Y, Okada S, Minamino T, Terasaki F, Kitaura Y and Komuro I: ATF6 is important under both pathological and physiological states in the heart. *J Mol Cell Cardiol* 49: 113-120, 2010.
- Adachi Y, Yamamoto K, Okada T, Yoshida H, Harada A and Mori K: ATF6 is a transcription factor specializing in the regulation of quality control proteins in the endoplasmic reticulum. *Cell Struct Funct* 33: 75-89, 2008.
- Boyce M, Bryant KF, Jousse C, Long K, Harding HP, Scheuner D, Kaufman RJ, Ma D, Coen DM, Ron D and Yuan J: A selective inhibitor of eIF2 α dephosphorylation protects cells from ER stress. *Science* 307: 935-939, 2005.
- Boyd JD, Lee-Armandt JP, Feiler MS, Zaarur N, Liu M, Kraemer B, Concannon JB, Ebata A, Wolozin B and Glicksman MA: A high-content screen identifies novel compounds that inhibit stress-induced TDP-43 cellular aggregation and associated cytotoxicity. *J Biomol Screen* 19: 44-56, 2014.
- Mori T, Saito F, Yoshino T, Takeyama H and Matsunaga T: Reporter gene assay against lipophilic chemicals based on site-specific genomic recombination of a nuclear receptor gene, its response element, and a luciferase reporter gene within a stable HeLa cell line. *Biotechnol Bioeng* 99: 1453-1461, 2008.
- Gasparetto M, Gentry T, Sebt S, O'Bryan E, Nimmanapalli R, Blaskovich MA, Bhalla K, Rizzieri D, Haaland P, Dunne J and Smith C: Identification of compounds that enhance the anti-lymphoma activity of rituximab using flow cytometric high-content screening. *J Immunol Methods* 292: 59-71, 2004.
- Starkuviene V and Pepperkok R: The potential of high-content high-throughput microscopy in drug discovery. *Br J Pharmacol* 152: 62-71, 2007.
- Feng Y, Mitchison TJ, Bender A, Young DW and Tallarico JA: Multi-parameter phenotypic profiling: using cellular effects to characterize small-molecule compounds. *Nat Rev Drug Discov* 8: 567-578, 2009.
- Giuliano KA, Haskins JR and Taylor DL: Advances in high content screening for drug discovery. *Assay Drug Dev Technol* 1: 565-577, 2003.
- Liu CL, Li X, Hu GL, Li RJ, He YY, Zhong W, Li S, He KL and Wang LL: Salubrinal protects against tunicamycin and hypoxia induced cardiomyocyte apoptosis via the PERK-eIF2 α signaling pathway. *J Geriatr Cardiol* 9: 258-268, 2012.